ACS Catalysis

Research Article

pubs.acs.org/acscatalysis

Single- and Double-Coordination Mechanism in Ethylene Tri- and Tetramerization with Cr/PNP Catalysts

George J. P. Britovsek,*[,†] David S. McGuinness,*[,‡] Tanita S. Wierenga,[‡] and Craig T. Young[†]

[†]Department of Chemistry, Imperial College London, Exhibition Road, South Kensington, London SW7 2AZ, United Kingdom

[‡]School of Physical Sciences−Chemistry, University of Tasmania, Private Bag 75, Hobart 7001, Australia

Supporting Information

ABSTRACT: The mechanism of ethylene trimerization and tetramerization with a chromium−diphosphinoamine (Cr−PNP) catalyst system has been studied with combined experimental and theoretical methods. Of the total product output, 1-octene, cyclopentanes, *n*-alkanes, and higher (C_{10+}) olefins are formed with a fractional (~1.4) order response to ethylene concentration, whereas 1-hexene formation is approximately first-order in ethylene. Theoretical studies suggest a mechanism involving a cationic monometallic catalyst in Cr(I) and Cr(III) formal oxidation states. A key feature of the developed model is the occurrence of a double-coordination mechanism in which a bis(ethylene) chromacyclopentane intermediate is responsible for 1-octene formation as well as the other coproducts that have a greater than first-order response to ethylene. In contrast, 1-hexene is formed primarily from a mono(ethylene) chromacyclopentane intermediate. The selectivity of catalysis is governed by the competition between single- and double-coordination pathways. The mechanistic model developed displays excellent correlation with experimental observations and is able to fully explain the formation of all products generated with this catalyst.

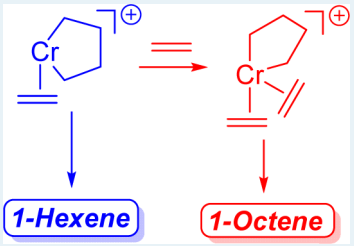

KEYWORDS: *oligomerization, trimerization, tetramerization, chromium, catalysis, reaction mechanism*

1. INTRODUCTION

The oligomerization of ethylene to short-chain linear α-olefins (LAOs) continues to be an area of much research interest in both industry and academia.[1−4] The first three homologues of the series, 1-butene, 1-hexene, and 1-octene, are used as comonomers for the production of polyethylene and represent the largest volume use of LAOs. For this reason, there is ongoing interest in catalysts that selectively produce these short-chain LAOs, particularly 1-hexene and 1-octene.[5−9] A generalized mechanism for selective formation of 1-hexene and 1-octene is shown in Scheme 1 and is thought to involve metallacycle formation, ethylene insertion, and a termination process to produce the α-olefin. The selectivity of the process is thought to be controlled by the relative stability of the different-sized metallacycles, in particular whether they terminate to give the α-olefin product or grow by further insertion of ethylene.

Scheme 1. Metallacyclic Mechanism for Ethylene Trimerization and Tetramerization

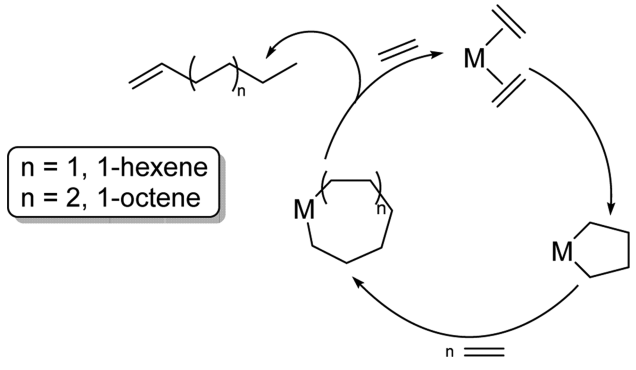

The majority of catalysts developed for this reaction are based upon chromium, and from these, the selective formation of 1-hexene (trimerization) is most common.[5,6,8] Far fewer systems are capable of producing 1-octene (tetramerization) with high selectivity.[10−14] The most successful system for combined trimerization and tetramerization was reported by researchers from Sasol in 2004 and consists of a chromium source, methylaluminoxane (MAO) cocatalyst, and a diphosphinoamine (PNP) ligand of structure **I** (Chart 1).[10] This system has recently been commercialized by Sasol on a 100 kt per annum scale. One notable aspect of this catalyst is the ability to control the relative hexene-to-octene selectivity through ligand modification; bulky groups favor 1-hexene, whereas less encumbered ligands favor 1-octene.[15]

Chart 1

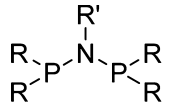

I

Received: May 11, 2015
Published: May 28, 2015

DOI: 10.1021/acscatal.5b00989
ACS Catal. 2015, 5, 4152−4166

Table 1. Ethylene Oligomerization with Cr/PNP/MAO[a]

run	C_2H_4 (bar)	product[b] (g)	activity[b,c]	PE (wt %)	1-C_6 (wt %)	1-C_8 (wt %)	1-C_{10+} (wt %)	cyclopent. (wt %)	*n*-alkanes (wt %)	C_{10}–C_{14} co-olig (wt %)
1	10	3.13	12,031	3.9	23.3	61.0	2.4	7.2	0.4	1.2
2	20	6.87	26,441	6.2	14.3	66.1	4.1	7.0	0.4	1.4
3	30	12.69	48,815	5.0	12.0	67.2	5.7	7.4	0.6	1.3
4	40	19.19	73,826	5.7	8.5	68.2	7.8	7.3	0.9	1.3
5	50	28.29	108,803	7.5	8.5	65.1	8.5	7.4	1.0	1.1
6[d]	30	16.56	63,695	4.7	12.2	65.9	6.0	7.5	0.6	1.3

[a]Conditions: 10 μmol $[CrCl_3(thf)_3]$, 10 μmol $Ph_2PN(^iPr)PPh_2$, 3 mmol MAO, toluene 100 mL, 30 °C, 30 min. [b]Product yields and activities include polyethylene. [c]g(product)·g(Cr)$^{-1}$·h^{-1}. [d]1-Pentene (9 mL, 82 mmol) added. Total C_9,C_{11} and C_{13} alkene isomers: 0.8 wt %.

Although progress has been made understanding the mechanism of this catalyst,[16−27] many questions remain. The formal oxidation state of the active catalyst is not known with certainty, with the cycle shown in Scheme 1 possibly shuttling between Cr(I)−Cr(III) or Cr(II)−Cr(IV) intermediates. The factors controlling 1-hexene versus 1-octene selectivity, or even why this catalyst produces 1-octene whereas most systems only produce 1-hexene, is also not well understood. The formation of a greater range of coproducts with this catalyst, as compared with most trimerization systems that produce 1-hexene relatively cleanly, also requires explanation. In attempting to answer these questions, we have undertaken a detailed experimental and theoretical investigation of the Cr/PNP/MAO catalyst system. Our first results in this regard, which included benchmarking to ascertain suitable theoretical methods and addressed the question of oxidation states, was recently published.[28] Herein, we report a full study of the system aimed at removing much of the uncertainty surrounding this catalyst.

In this work, we have attempted to provide a complete mechanistic proposal, which explains all experimental observations made with this catalyst. In the first section of the paper, the experimental results of the oligomerization system are analyzed in detail to establish what the mechanistic proposal must account for. In the second part, theoretical techniques are used to develop a mechanistic model, which can account for all observed products of the oligomerization process. Finally, the experimental findings are correlated to the developed theoretical model.

2. RESULTS AND DISCUSSION

2.1. Experimental Observations. Ethylene trimerization and tetramerization produces, in addition to 1-hexene and 1-octene, a range of additional coproducts in varying amounts. The formation of most of these coproducts has not yet been adequately rationalized, but we reasoned their mode of formation and relationship to 1-hexene and 1-octene may provide useful mechanistic insight. A reasonably complete account of the identity of all products formed by this system has previously been provided by researchers from Sasol;[17] however, a detailed analysis of their distribution, response to ethylene pressure, and correlation to 1-hexene or 1-octene formation was not reported. To carry out such an analysis, we have conducted ethylene oligomerization experiments with a representative Cr/PNP/MAO catalyst system. This was composed of an in situ-formed catalyst of ligand **I** (R = Ph, R′ = ^{i}Pr), $[CrCl_3(thf)_3]$ and MAO (1:1:300) in toluene. All experiments were conducted with a chromium loading of 10 μmol in 100 mL total volume of toluene ([Cr] = 100 μM) at 30 °C and constant pressure. Optimization of the system, chiefly much lower catalyst loadings (but also ligand, solvent, chromium source, and temperature) can lead to much improved activities with this catalyst,[11,29−31] but that was not the remit of this work. Our aim was rather to generate reliable and reproducible data on each of the products. The conditions employed herein achieve this and in most cases lead to reliable analysis of all products of interest.

A summary of the results of ethylene oligomerization at different pressures is presented in Table 1 (a more detailed breakdown of the results can be found in the Supporting Information). In general terms, our results are quite consistent with earlier reported results with this system.[17] Aside from C_{10+} α-olefins, the significant coproducts produced, cyclopentanes, *n*-alkanes and C_{10}−C_{14} co-oligomers, are illustrated in Scheme 2. The cyclopentane products are composed predominately of

Scheme 2. Coproducts Formed during Ethylene Trimerization/Tetramerization

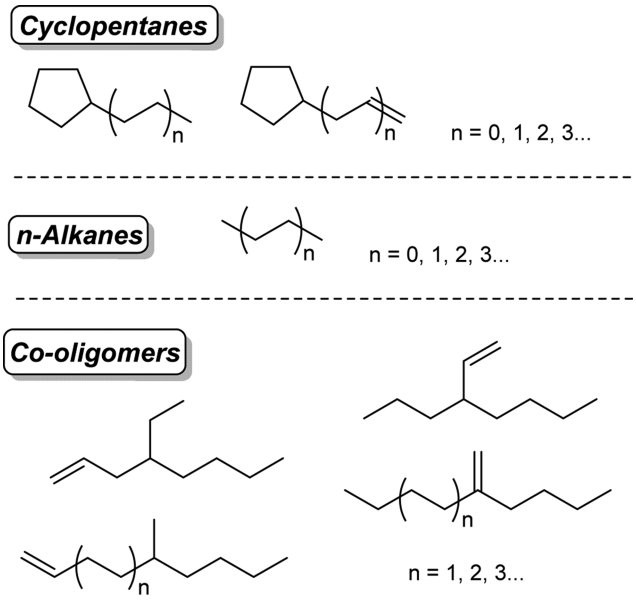

methyl cyclopentane and methylene cyclopentane, with lesser amounts of the longer chain cyclopentane derivatives. Within each carbon number fraction of these cyclopentanes, the ratio of saturated to unsaturated products is approximately 1:1. Both the cyclopentane and the *n*-alkane products follow a Schulz−Flory distribution, which is numerically analyzed later (Section 2.3). It should be noted that cyclopentane formation appears to be in some way associated with the tetramerization process; these products are observed only with catalysts that produce 1-octene, not with catalysts that are selective for 1-hexene

DOI: 10.1021/acscatal.5b00989
ACS Catal. 2015, 5, 4152−4166

formation. This is despite the fact that the most abundant cyclopentanes are the C_6 products methyl cyclopentane and methylene cyclopentane.

A number of proposals have been suggested for formation of the cyclopentane products,[17,32] but a complete rationalization is lacking. The *n*-alkane products formed in ethylene oligomerization processes can potentially result from chain transfer reactions with the MAO cocatalyst.[33] We note, however, that odd-numbered *n*-alkanes are absent in our experiments, which would be expected if significant chain transfer with $AlMe_3$/MAO was taking place. The formation of C_{10}-C_{14} co-oligomers is generally explained by cotrimerization and cotetramerization of 1-hexene and 1-octene with ethylene. Experiments involving incorporation of externally added α-olefins support this idea.[17,19,34,35] This effect has been confirmed under our conditions by adding 1-pentene to the reaction; the formation of branched C_9, C_{11}, and C_{13} products is observed (see run 6, Table 1). The addition of 1-pentene (9 mL, 82 mmol) does not affect the product distribution (c.f. run 3), but 0.9 mmol of C_9, C_{11}, and C_{13} alkene coproducts are formed (in addition to the C_{10}, C_{12}, and C_{14} co-oligomers), which corresponds to 1.1 mol % 1-pentene incorporation. Furthermore, the C_{10}−C_{14} alkene isomer fraction derived from 1-hexene and 1-octene incorporation is not affected by the addition of this large amount of 1-pentene.

A number of kinetics studies on this oligomerization system have shown that the overall reaction is first-order with respect to chromium and displays an order of ∼1.6 with respect to ethylene pressure (ethylene pressure has been found to be a reliable proxy for concentration in solution).[36,37] The latter is made up of an approximately first-order ethylene dependence for 1-hexene formation and a second-order ethylene dependence for 1-octene formation.[37] One study concluded that the effect of ethylene concentration on the minor products was too small to draw any firm conclusions, and the formation of the cyclopentane products was independent of ethylene concentration.[38] We have also found that 1-octene displays a partial second-order dependence on ethylene pressure, and 1-hexene formation follows kinetics approaching first-order with respect to ethylene. Our conclusions with respect to the coproducts differ, however. Although the data in Table 1 would seemingly support the conclusion that the formation of cyclopentanes is unaffected by ethylene pressure, comparison of selectivities in this way tends to mask the true response of each product class to ethylene concentration. By analyzing the absolute amount of each product formed as a function of ethylene pressure, we find that in addition to 1-octene, the cyclopentanes, *n*-alkanes and higher LAOs (1-decene and up) also display clear evidence for a second-order contribution to their formation (with respect to ethylene).

For a rate equation of the form $r = k[\mathrm{Cr}][C_2H_4]^n$, a plot of the logarithm of the rate (or amount of product formed within a given time) versus the logarithm of ethylene pressure should give a linear relationship in which the slope equates to the order in ethylene. Such an analysis is shown in the Supporting Information, Figure S1. This approach gives an overall order in ethylene of 1.3 for our system, with the orders for the individual product classes varying. For 1-hexene, an order of 0.71 (R^2 = 0.91) is found, which could indicate first-order kinetics. Fitting the data for 1-hexene to a simple first-order relationship, $r = k \cdot P_{\mathrm{ethylene}}$, leads to a fit with R^2 = 0.91, which is not substantially worse (Figure 1a). An order of 1.4 for 1-octene and 1.3 for the cyclopentanes is found, with the *n*-alkanes and C_{10+} LAOs

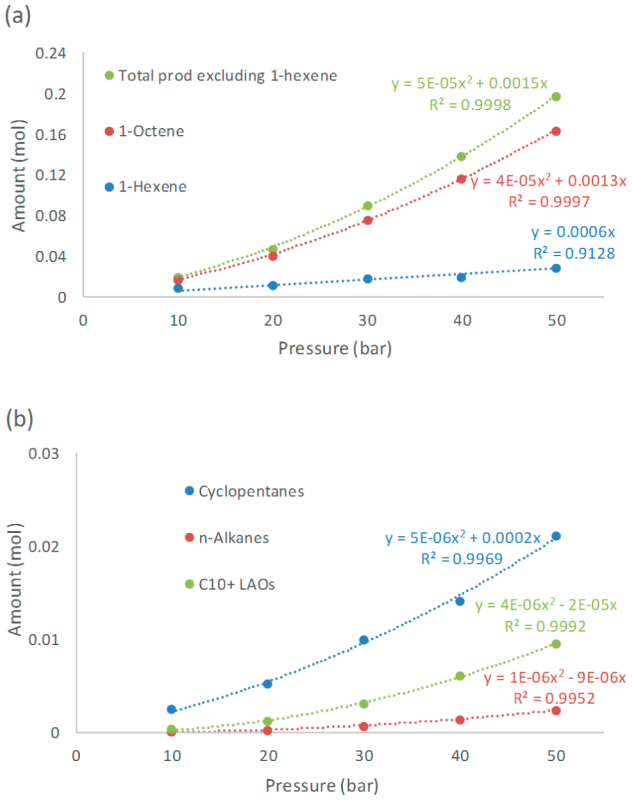

Figure 1. Amount of (a) total liquid products excluding 1-hexene, 1-hexene, and 1-octene, and (b) cyclopentanes, alkanes, and higher LAOs formed as a function of ethylene pressure.

displaying an apparent order close to 2. The values for the products other than 1-hexene indicate mixed-order kinetics, and for reasons that will be discussed below, a rate equation of the form $r = k[C_2H_4]^2 + k'[C_2H_4]$ may be a better description. In this case, it is more appropriate to fit the data to a quadratic function, as illustrated in Figure 1. For the most abundant products, 1-octene and the cyclopentanes, this treatment leads to an excellent fit to the experimental data, in which the two terms indicate both first- and second-order components to their formation. The contribution of each term is illustrated graphically in Figures S2 and S3. At low ethylene pressure, the first-order term is dominant, whereas at higher pressures, the second-order process becomes the major contributing path to product formation. For the less abundant products, *n*-alkanes and higher LAOs, an excellent fit is also obtained, although it is noted that the first-order term is slightly negative, probably due to imperfect data and noting that these products are present in very small amounts (the alkanes expected to be most abundant, ethane and butane, are not readily quantifiable and are therefore not included in the analysis). Plots for each individual carbon number fraction of the cyclopentanes and *n*-alkanes are shown in Figures S4−S9). From this analysis, we conclude that 1-octene, the cyclopentanes, the alkanes, and C_{10+} LAOs might be formed by processes that are both first- and second-order with respect to ethylene (although there are alternate explanations for the observed kinetics, as discussed later). As we show below, this finding may be correlated to their mechanism of formation.

2.2. Theoretical Studies. We have recently published a theoretical benchmarking study and assessment of catalyst oxidation state for the Cr/PNP/MAO catalyst system, and a

DOI: 10.1021/acscatal.5b00989
ACS Catal. 2015, 5, 4152−4166

full rationale for the model catalyst and theoretical methods employed is contained therein.[28] Briefly, this work revealed that the system is challenging from a theoretical perspective but that several local density functionals (BP86, BPW91, and M06L) lead to acceptable results. The M06L functional was employed to study the early stages of oligomerization and is the method used in the present work (see the Supporting Information for full details of theoretical methods). The conclusion from the benchmarking study was that the cationic active catalyst shuttles between Cr(I) and Cr(III) formal oxidation states, with a Cr(II)−Cr(IV) cycle less preferred both kinetically and thermodynamically. A smaller version of ligand **I** where $R = R' =$ Me was used in the study. This was rationalized on the basis that such ligands have been shown to lead to active trimerization/tetramerization catalysts,[10,39] even though P-aryl substitution is more typical. The same ligand substitution has been employed in the calculations in this work.

Metallacycle Formation. The starting point for metallacylic oligomerization is taken as the $[(PNP)Cr(H_2C{=}CH_2)]^+$ complex (^{6}**1**, Chart 2) in the sextet spin state ($S = 5/2$). A

Chart 2

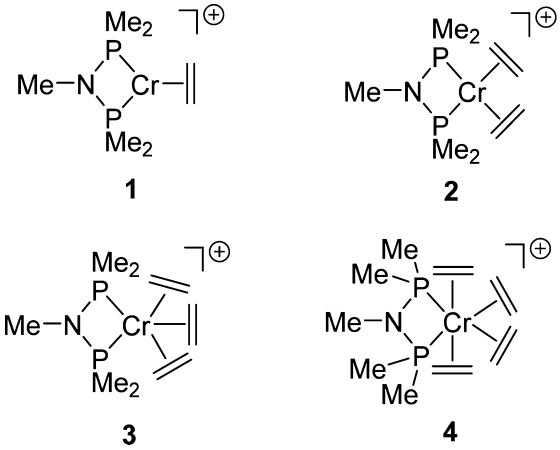

facile activation route leading to such Cr(I) olefin complexes was demonstrated previously.[28] All energies reported throughout this work are relative to this complex, balanced for ethylene, unless otherwise stated. Coordination of additional ethylene leads to $[(PNP)Cr(H_2C{=}CH_2)_n]^+$ cations **2**−**4** ($n = 2$−4) from which metallacycle formation can occur by coupling of two ethylene ligands. The most stable spin state calculated for each complex depends upon the number of coordinated ethylenes, with **1** and **2** the most stable in the sextet state, and **3** and **4** preferring the quartet state. The addition of more ethylene ligands results in a stronger ligand field and consequent electron pairing to give a lower spin state. A complete analysis of relative spin state energies for intermediates in different oxidation states was included in our previous benchmarking study of this system.[28]

The various routes to chromacyclopentane formation are shown in Figure 2.[40] It is found that metallacycle formation in the sextet state is associated with a very high barrier (shown in gray in Figure 2). This is perhaps not surprising because the process involves transformation from a formally Cr(I) ethylene complex (d^5) to a Cr(III) metallacycle (d^3). So far as such formalism is an appropriate description, a sextet configuration for a d^3 complex is expected to be much higher in energy than the quartet, and this destabilization also applies to the transition state structure. A significantly more favorable route to metallacycle formation involves spin crossing to the quartet state, followed by ethylene coupling. The sextet-to-quartet minimum energy crossing points[41] for the two lowest-energy Cr−ethylene complexes have been located (^{6}**2** → ^{4}**2** and ^{6}**3** → ^{4}**3**). Metallacycle formation from the bis(ethylene) complex ^{4}**2** (black pathway) is calculated to be very similar in energy to that via the tris(ethylene) complex ^{4}**3** (blue), going via **TS2-6** at 9.1 kcal·mol^{-1} or **TS3-7** at 9.7 kcal·mol^{-1}. Metallacycle formation via the tetra(ethylene) complex ^{4}**4** (red path) is a little more difficult, with **TS4-5** at 12.2 kcal·mol^{-1}, but given the uncertainty in the calculated energies,[28] this pathway is also definitely a possibility. Transition structure **TS4-5** leads to complex **5** with trans ethylene ligands. Isomerization could lead to a more stable complex with cis ethylene ligands (see below), or alternatively, ethylene dissociation could yield complex **7**.

Taking into account the relatively small calculated energy differences among the three Cr(ethylene)$_n$ complexes ($n = 2$−4) and the transition structures, it is entirely conceivable that multiple pathways for metallacycle formation are operative, and this will be affected by the concentration of ethylene in solution.

Reactions of Chromacyclopentane. One of the key features of selective oligomerization via metallacycles is thought to be the relative stability of metallacyclopentanes toward termination.[42−44] This is attributed to the constrained geometry of the 5-membered ring, which hinders β-hydride transfer such that metallacycle expansion via ethylene insertion becomes preferred.[45−47] Each of the four possibilities (a−d) summarized in Scheme 3 has been investigated herein. Path a corresponds to β-H transfer to chromium, followed by C−H reductive elimination to produce 1-butene. Path b is the concerted route to 1-butene, involving β-H transfer to the α'-C in one step. Path c, which has hitherto not been considered, to our knowledge, involves β-H transfer to a coordinated ethylene, followed by transfer of a β-H back to the α'-C of the butenyl group. Finally, path d corresponds to ethylene insertion to expand the metallacycle to chromacycloheptane species.

Because complex $[(PNP)Cr(C_4H_8)(H_2C{=}CH_2)]^+$, **7**, can in principle undergo each of the processes shown in Scheme 3, this species was chosen to study the relative energetics of each. The free energy surface is shown in Figure 3. Ethylene insertion to expand the metallacycle (black pathway) has a relatively low free-energy barrier (8.1 kcal·mol^{-1} from **7**). In contrast, each of the processes involving β-H transfer have considerably higher energy transition structures, the highest of those located being β-H transfer to ethylene (red pathway). Transfer of the β-H to chromium carries less of a penalty, but is followed by a higher-energy C−H reductive elimination of 1-butene (blue path). Despite repeated attempts, we were unable to locate a transition structure corresponding to concerted β-H → α' transfer (Scheme 3, route b). We[48] and others[47,49] have previously located this transition structure for titanium complexes, and therefore, the approximate geometric parameters are known. Constraining the geometry in such a manner does lead to a primary (largest) imaginary frequency consistent with the process of interest, but attempted transition structure optimization from there always led to either **TS7-10**, **TS7-9**, or **TS9-11** (depending upon the arrangement of the other ligands). It is noted that optimization to these transition structures, which are already high, was a downhill process in each case. Others have also reported that this transition

DOI: 10.1021/acscatal.5b00989
ACS Catal. 2015, 5, 4152−4166

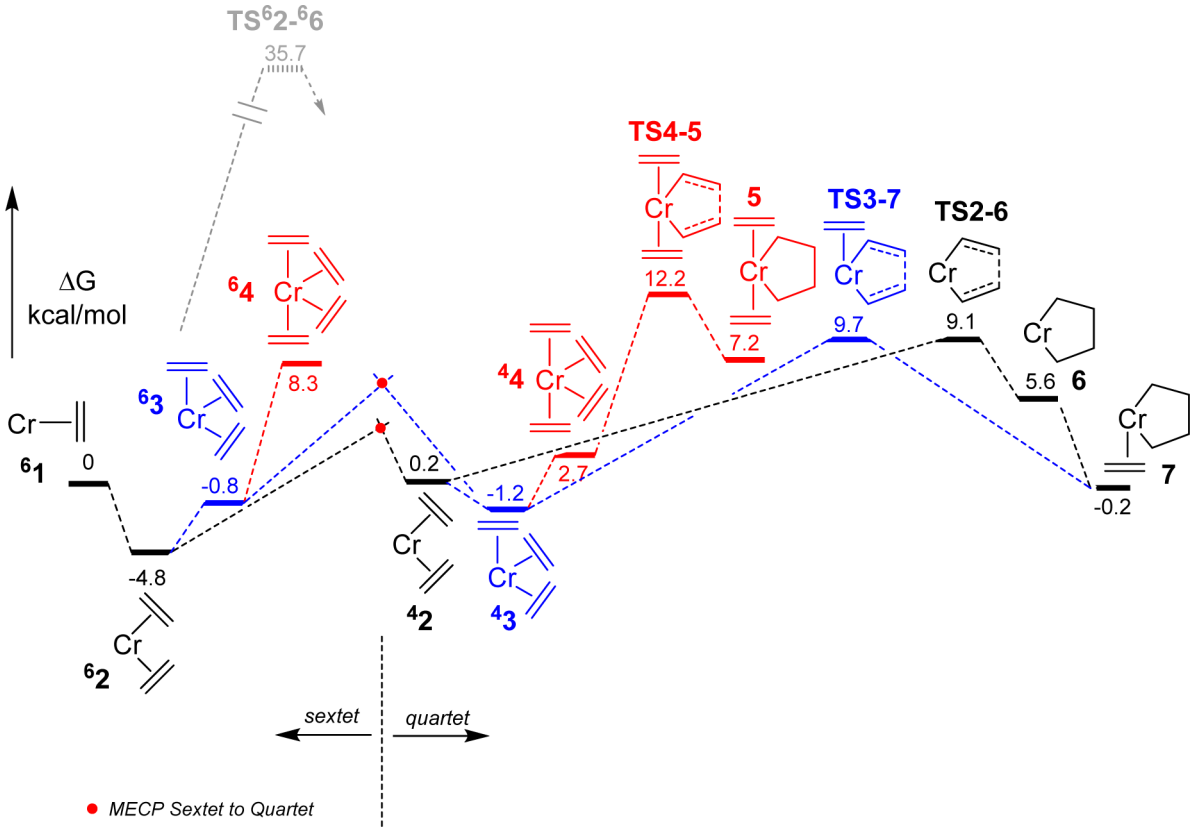

Figure 2. Energy profiles for metallacyclopentane formation via various Cr(ethylene)$_n$ intermediates. All stationary points shown are cationic. The relative Gibbs free energies (ΔG) obtained from M06L/BS2//M06L/BS1 calculations are given in kcal·mol^{-1}. The minimum energy crossing point energy levels are derived from M06L/BS1 electronic energies.

Scheme 3. Further reactions (a-d) of chromacyclopentanes

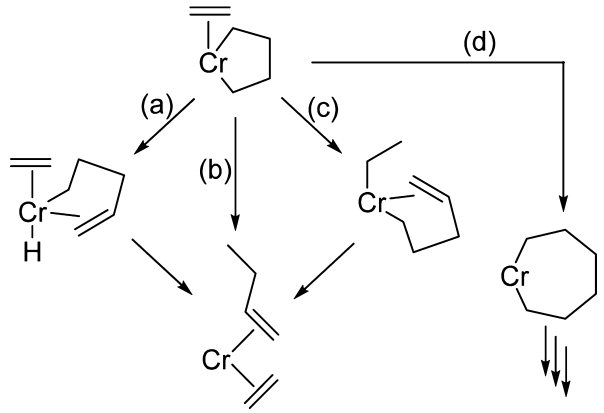

structure could not be located for related chromium catalysts.[50,51]

It is clear that, as found in other systems, the metallacyclopentane ring in Cr(III)-PNP complexes is relatively stable against termination to 1-butene. Hence, metallacycle expansion via **TS7-8** at 7.9 kcal·mol^{-1} (route d) to a chromacycloheptane (**8**) will be kinetically preferred, and the formation of appreciable amounts of 1-butene is therefore neither expected nor experimentally found.

Reactions of Chromacycloheptane ***8.*** In this section, we consider further potential reaction pathways of the chromacycloheptane complex **8**, which does not at this stage contain coordinated ethylene. Uptake of additional ethylene and subsequent reactions are considered in detail in the next section.

Prior theoretical work on other trimerization systems suggests that the most favorable route to 1-hexene formation from metallacycloheptanes is via concerted β-H transfer to the α'-C.[45,47,48] This is likewise predicted to be the case with complex **8**, as shown in Figure 4 (black trace via **TS8-12**). The alternative, stepwise β-H elimination and reductive elimination (blue trace via **TS8-14** and **TS14-12**) is calculated to have a slightly higher barrier. A number of other reaction path possibilities were also considered. First, C−C reductive elimination to produce cyclohexane (red path) has a rather high barrier compared with 1-hexene formation. This is consistent with experiment because cyclohexane formation is not observed with this system (nor with any other trimerization catalyst, to our knowledge). Another process modeled was back-biting insertion from **14** to produce [(PNP)CrH-(methylcyclopentyl)]$^+$ **15**, and subsequent reductive elimination of methylcyclopentane.[52] Although such a process might offer a partial explanation for the cyclic products observed with this catalyst, the barrier via **TS14-15** is higher than that for 1-hexene formation. In addition, we show below an alternate process that is more competitive and can account for all of the cyclopentane products observed. Therefore, the reactivity of **15** was not probed any further.

The findings presented in Figure 4 suggest that, in the absence of coordinated ethylene, chromacycloheptane **8** will lead selectively to 1-hexene formation. With regard to a rate-determining step for 1-hexene formation, we note that the overall barrier for metallacycle formation (Figure 2, ^{6}**2** → **TS2-**

DOI: 10.1021/acscatal.5b00989
ACS Catal. 2015, 5, 4152−4166

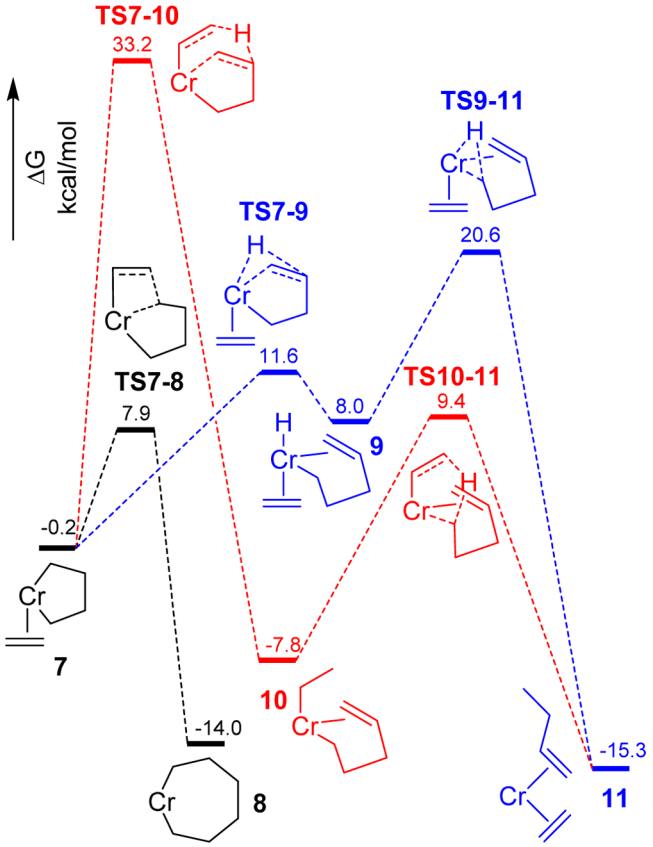

Figure 3. Energy profiles for three further reactions from [(PNP)Cr-(C_4H_8)(ethylene)]$^+$ (**7**). All stationary points shown are cationic. The relative Gibbs free energies (ΔG) obtained from M06L/BS2//M06L/BS1 calculations are given in kcal·mol^{-1}. a = blue, c = red, d = black.

6, 13.9 kcal·mol^{-1}) is calculated to be the same as that for metallacycle termination (Figure 4, **8** → **TS8-12**, 13.9 kcal·mol^{-1}). It is therefore difficult to suggest which process is rate-determining in this case. Given that 1-hexene formation is found to be approximately first-order in ethylene concentration, metallacycle formation (which involves ethylene) might be in control, whereas the rate of termination (**TS8-12**) should be independent of ethylene concentration. A full discussion of the correlation between theory and the observed kinetics is included later.

Formation and Reactions of Chromacyclononanes. It has been shown above that in the absence of additional coordinated ethylene, 1-hexene formation should be the primary product resulting from chromacycloheptane termination. We consider now the possibility of coordination of further ethylene and metallacycle expansion.

Because it is believed that 1-octene results from a metallacyclononane intermediate and its formation has a component of second-order dependence on ethylene concentration, it seems likely that chromacyclononane formation would display similar kinetics. Two related mechanisms have in the past been proposed to account for a second-order ethylene dependence in conventional (acyclic chain growth) oligomerization and polymerization via a Cossee−Arlman mechanism. The first is the "trigger mechanism"[53] in which insertion of a first monomer is triggered by an incoming (but not completely coordinated) second monomer. A variant on this is the double-coordination mechanism,[54,55] in which two monomers are fully coordinated to the metal center prior to insertion. Under both of these proposals, the first monomer will not insert as long as a second monomer is not interacting with the metal center.

Accordingly, we consider first the reactivity of the complex [(PNP)Cr(C_4H_8)(H_2C═CH_2)$_2$]$^+$. Two coordination isomers of this cation exist: complex **5** from Figure 2 with two ethylene ligands in trans axial positions and the isomer complex **17** with cis (axial−equatorial) ethylene ligands, which represents the most stable structure (Chart 3).

One possibility that seemed to warrant investigation was the synchronous migratory insertion of both ethylene units in one step (Scheme S2). Such a mechanism has hitherto not been proposed, to our knowledge, but essentially represents the limiting extreme of the trigger or double-coordination mechanisms. Investigation of this possibility is detailed in the Supporting Information and was ultimately found to be uncompetitive with stepwise single insertions.

A single insertion of ethylene in complex **17** leads to [(PNP)Cr(C_6H_{12})(H_2C═CH_2)]$^+$ (**18**), a chromacyclononane with one coordinated ethylene ligand. We focus here on ring expansion from **17** because it is lower in energy than complex **5** and also has the lowest barrier for the first insertion of ethylene. In fact, there are a number of possibilities for the first insertion reaction of **17**, depending on which ethylene inserts into which Cr−alkyl bond, and each of these leads to a different isomer or conformer of **18**. In addition, the 7-membered ring can adopt different conformations (in most cases including an agostic Cr···H interaction), and even the orientation of the ethylene ligand leads to different local minima. We have attempted to cover all possibilities, and the result is a rather complex picture for the formation and interconversion of the conformers and isomers of **18**, which is illustrated in Figure 5.

A range of possibilities for further reaction of **18** were also discovered and these are indicated in Figure 5. The reaction pathway shown in black includes the first insertion of ethylene (via **TS17-18a**, migration of alkyl-*trans*-P to ethylene-*trans*-P), followed by the route to interconversion of the various conformers/isomers of **18** (**18a** → **18g**). Alternative, higher-energy, transition structures for the first insertion are shown in gray (**TS17-18e** and **TS17-18f**). Transition structures for insertion of the second ethylene unit to produce chromacyclononanes are indicated in blue, and β-hydride transfer reactions (β-H transfer to ethylene, α'-C, or to Cr) are illustrated in red.

The lowest-energy route to **18** is via **TS17-18a** (6.1 kcal·mol^{-1}), with the next being **TS17-18f** (11.8 kcal·mol^{-1}) to produce isomer **18f** with the alkyl groups trans to the phosphines. For comparison, the first insertion from **5** also has a barrier of 11.8 kcal·mol^{-1} and leads to a complex of very similar structure and energy to **18a**. **TS17-18a** is sufficiently below the other insertion transition structures that it is likely to be the primary route to complex **18**. From **18a**, there is a low barrier for conformational isomerization to give **18b**, which contains a β-hydride agostic interaction and is the most stable form of **18** (the transition structure energies for conformer/isomer interconversion are given in italics in Figure 5).[56] Most of the barriers for conformational change are rather low, as might be expected. The highest barrier corresponds to coordination isomerization from **18e** to **18f**, but this, too, is below each of the transition structures for further reaction (insertion or β-H transfer). It therefore seems possible that the various forms of complex **18** are in thermodynamic equilibrium.

Complexes **18a**, **c**, **e**, **f** and **g** are all connected to transition structures for metallacycle expansion to a chromacyclononane (blue). The lowest of these at −4.5 kcal·mol^{-1} is linked with

DOI: 10.1021/acscatal.5b00989
ACS Catal. 2015, 5, 4152−4166

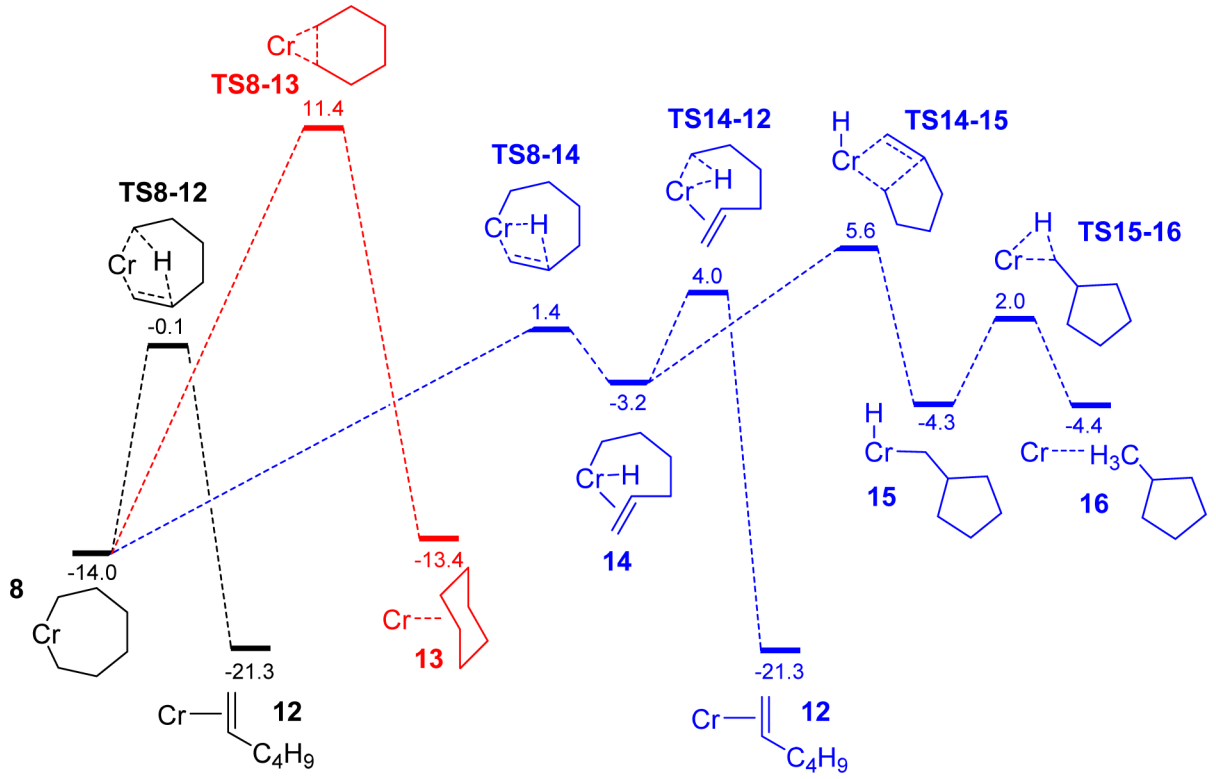

Figure 4. Energy profiles for further reactions from $[(PNP)Cr(C_6H_{12})]^+$ (**8**). All stationary points shown are cationic. The relative Gibbs free energies (ΔG) obtained from M06L/BS2//M06L/BS1 calculations are given in kcal·mol^{-1}.

Chart 3

complex **18f**. Most of the transition structures for β-hydride transfer reactions are clustered at a similar energy (−1.4 to 0.1 kcal·mol^{-1}). The lowest corresponds to β-hydride transfer to ethylene. This highlights the pronounced effect of greater conformational freedom in larger metallacycles. In contrast to the metallacyclopentane complex **7** (Figure 3), where β-hydride transfer to ethylene has the highest barrier, in **18b**, this process has the next lowest transition structure after metallacycle expansion. We show below that the accessibility of this reaction pathway, which leads to a Cr(ethyl)(hexenyl) species, is a major reason for loss of 1-hexene and 1-octene selectivity with this catalyst.

To summarize the situation presented in Figure 5, from the bis(ethylene) complex **17**, insertion of one ethylene unit via **TS17-18a** is the most favorable route to complex **18**, for which there are a number of isomeric forms of different energies. Although these different isomers can also be accessed via higher-energy transition structures for the first insertion, the lowest energy pathway is via initial formation of **18a** and subsequent isomerization. The lowest energy process for further reactivity of **18** is metallacycle expansion from complex **18f**. It is therefore a reasonable conclusion that the primary product resulting from **18** will be a chromacyclononane complex.

In Figure 6, a simplified reaction surface is presented whereby only the lowest-energy isomer of **18** and the lowest transition structures for further reaction are shown (with omission of the isomerization details). These are compared with 1-hexene formation via **7** and **8**. It is also the case that **18** could form via ethylene coordination to complex **8**, and this possibility is also shown in Figure 6. In addition, the calculated barrier to 1-octene formation from chromacyclononane **19** is shown. It can be seen that addition of ethylene to **7**, to generate bis(ethylene) complex **17**, is calculated to be slightly exergonic and also that the barrier to insertion into **17** (**TS17-18a**) lies slightly lower than **TS7-8**. Hence, the theoretical results predict that formation of metallacycloheptane **18** will be favored over formation of **8**, dependent, of course, on the availability of ethylene. From complex **18**, formation of the 1-octene complex **20** results (blue pathway). Two possibilities for control of the reaction selectivity can be distinguished. First, if ethylene association/dissociation is very fast, then complexes **7** and **17** may be in thermodynamic equilibrium, where this equilibrium is partly controlled by the concentration of ethylene. Under these conditions, the selectivity to formation of **8** versus **18** is controlled by the position of this equilibrium and the transition structure barrier heights. This can be referred to as thermodynamic control. The second alternative is kinetic control, in which the fate of **7** is determined by the relative rates of ethylene insertion via **TS7-8** versus ethylene coordination to give **17**. In other words, a portion of complex **7** reacts to **8** faster than ethylene can coordinate. Again, this will be influenced by the concentration of ethylene. An equilibrium between **8** and **18**, also dependent on ethylene concentration, could likewise exists, but again, kinetic control could also dominate (rate of **8** → **12** versus **8** → **18**). We cannot at this stage determine which of these two alternatives represents the

DOI: 10.1021/acscatal.5b00989
ACS Catal. 2015, 5, 4152−4166

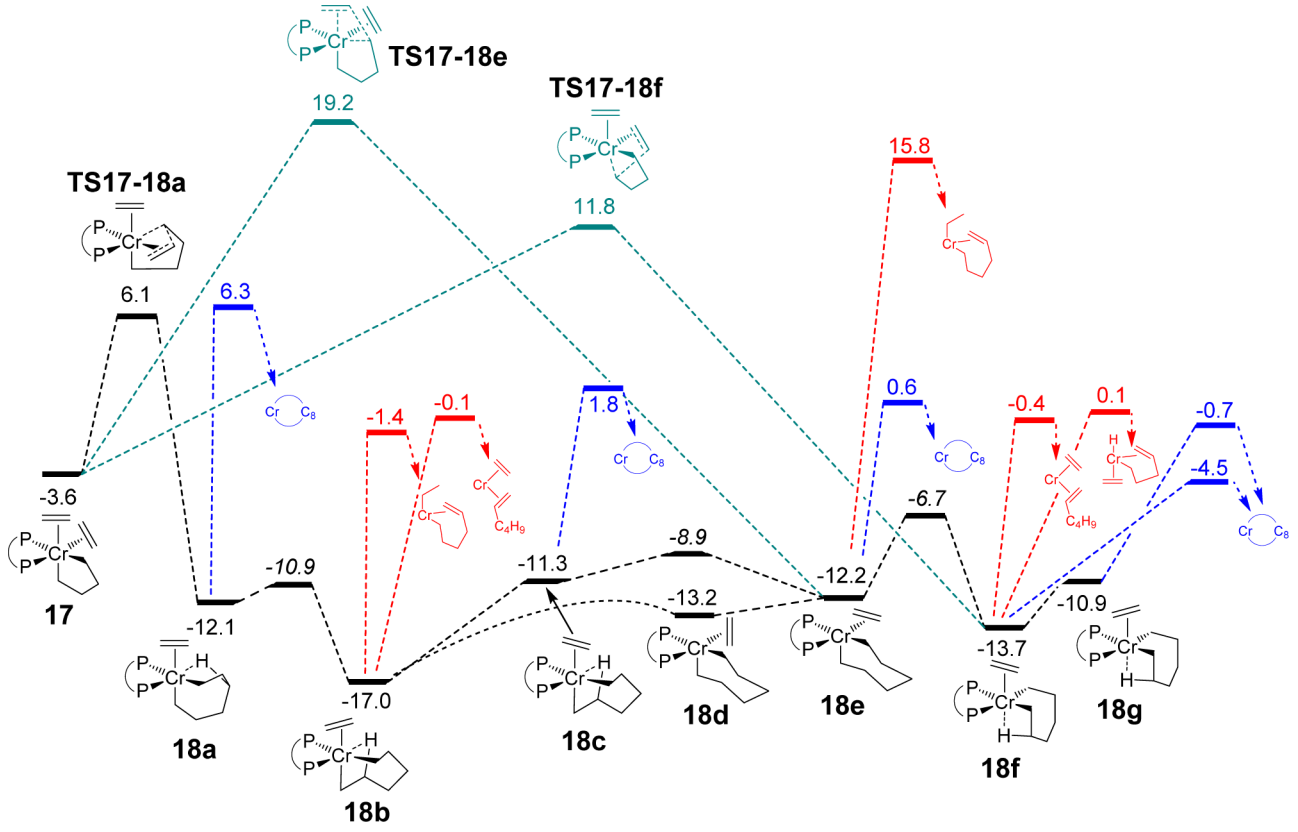

Figure 5. Energy profiles for metallacycle expansion and subsequent reactions from $[(PNP)Cr(C_4H_8)(ethylene)_2]^+$ (**17**). All stationary points shown are cationic. The relative Gibbs free energies (ΔG) obtained from M06L/BS2//M06L/BS1 calculations are given in kcal·mol^{-1}.

actual situation, but both can explain the selectivity of this system and its response to ethylene pressure. 1-Hexene will be formed predominately from **8**, whereas complex **18**, formed via either **17** or **8**, will give 1-octene.

The factors controlling the relative C_6 and C_8 selectivities are summarized in Scheme 4. In qualitative terms, these theoretical predictions provide a very good match to the experimentally observed results. The maximum 1-hexene selectivity will be observed at lower concentrations of ethylene, while at the same time, 1-octene formation is still preferred. An increase in ethylene pressure would lead to increased 1-octene formation at the expense of 1-hexene, as observed experimentally.

From Figure 6 and Scheme 4, two possible routes to 1-octene can be identified. A second-order ethylene dependence is reasonable for formation via bis(ethylene) complex **17**, whereas a first-order response would result via complex **8**. The relative contributions of each route will be dependent upon the ethylene concentration, and the mixed-order kinetics (Figure 1) can be understood in this context. This represents only one of a number of possibilities, however. As discussed below and in the Supporting Information, a mechanism in which 1-octene is formed *only* via bis(ethylene) complex **17** can also explain the observed kinetics. The trigger and double-coordination mechanisms mentioned at the beginning of this section propose that insertion will not occur unless two monomers are interacting with the metal center. This is not the case in the present system, however, where mono(ethylene) complex **7** can, and to an extent does, undergo insertion. Therefore, we are not dealing here with such a form of the double-coordination mechanism. Lemos and co-workers[54] proposed another possibility termed the single- and double-coordination mechanism, whereby both single- and double-monomer-coordinated complexes can be formed, and both are active toward insertion. The situation presented in Figure 6 appears to correspond closely to this model.

Metallacycle Expansion versus 1-Octene Formation. Further insertion of ethylene into the chromacyclononane ring, leading to larger metallacycles and higher α-olefins, is also a possibility that could compete with 1-octene formation. The formation of distributions of higher α-olefins via such a process has been observed in a number of cases (all of these are chromium-based catalysts)[57−61] and can be termed an extended metallacycle mechanism.[5] High 1-octene selectivity suggests that this process is not dominant for the catalyst of the present study, although it is noted that small amounts of higher linear α-olefins are observed that increase with ethylene pressure (Table 1). There are two possible routes to a chromacyclononane complex **22** with coordinated ethylene, as shown in Figure 7:[62] first, a double-coordination mechanism involving a chromacycloheptane complex **21**, and second, via coordination of ethylene to complex **19**. In contrast to the case above for a metallacyclopentane, the double coordination of ethylene and subsequent insertion (**TS21-22**) is quite unfavorable for a metallacycloheptane complex. Because there is no significant difference expected in the electronic environment (the ligation at chromium is equivalent), this is presumably for steric reasons. Coordination of ethylene to chromacyclononane **19** is slightly downhill; however, the transition structure for metallacycle expansion (**TS22-23**) is a little higher than that for 1-octene formation (**TS19-20**). This is opposite the situation in Figure 6, in which metallacyclononane formation is favored

DOI: 10.1021/acscatal.5b00989
ACS Catal. 2015, 5, 4152−4166

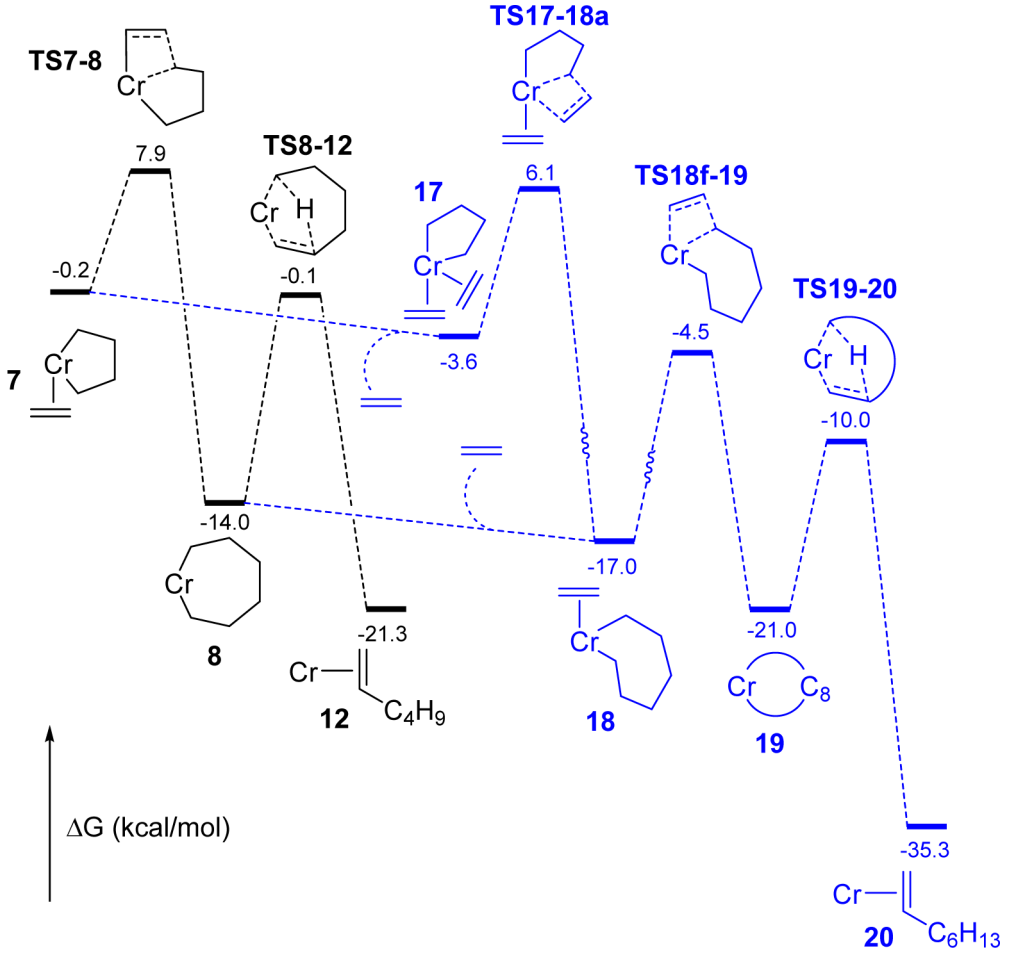

Figure 6. Condensed energy profiles for 1-hexene and 1-octene formation from $[(PNP)Cr(C_4H_8)(ethylene)]^+$ (**7**). All stationary points shown are cationic. The relative Gibbs free energies (ΔG) obtained from M06L/BS2//M06L/BS1 calculations are given in kcal·mol^{-1}.

Scheme 4. Control of 1-hexene/1-octene selectivity

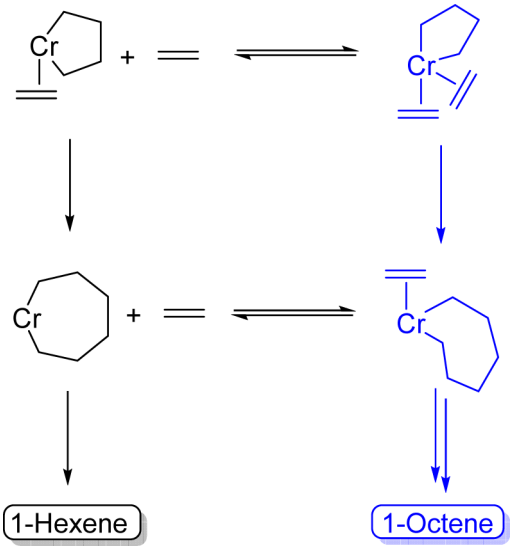

over 1-hexene formation. The selectivity for 1-octene with this catalyst can therefore be rationalized.

The prediction that the transition structure for 1-octene formation (**TS19-20**) and that for metallacycle expansion (**TS22-23**) are reasonably close in energy does support the idea that a distribution of higher α-olefins could result from a metallacyclic mechanism. This could lead to a modified Schulz−Flory distribution in which the products of termination from smaller metallacycles (in particular 1-butene, but also possibly 1-hexene) are less abundant than expected. Such a situation has, in fact, been observed previously, resulting from chromium catalysts supported by NHC ligands.[61]

Formation of Cyclopentanes and n-Alkanes. Of the various ways that complex **18** can react further, the process with the next-lowest barrier after ethylene insertion is β-hydride transfer to ethylene, which is also connected to the lowest-energy isomer of **18** (**18b**, Figure 5). Calculations on subsequent reaction possibilities suggest that this process is, indeed, accessible and does play a role in the oligomerization process. The β-hydride transfer reaction and subsequent processes are shown in Figure 8. The transfer reaction leads to (ethyl)(hexenyl)chromium complex **24**, in which the olefinic tail remains coordinated. From this point, we have located three possibilities for further reaction: C−C reductive elimination of 1-octene (**TS24-20**, red), β-hydride back-transfer to form 1-hexene (**TS24-25**, blue), and back-biting insertion of the olefinic tail to form a cyclopentylmethyl complex (**TS24-26**, black pathway). The binding arrangement of the hexenyl ligand in complex **24** appears well set up for back-biting insertion, and this process has a barrier considerably lower than the other possibilities. It seems likely, therefore, that cyclopentylmethyl complex **26** would be formed selectively from complex **24**. This

DOI: 10.1021/acscatal.5b00989
ACS Catal. 2015, 5, 4152−4166

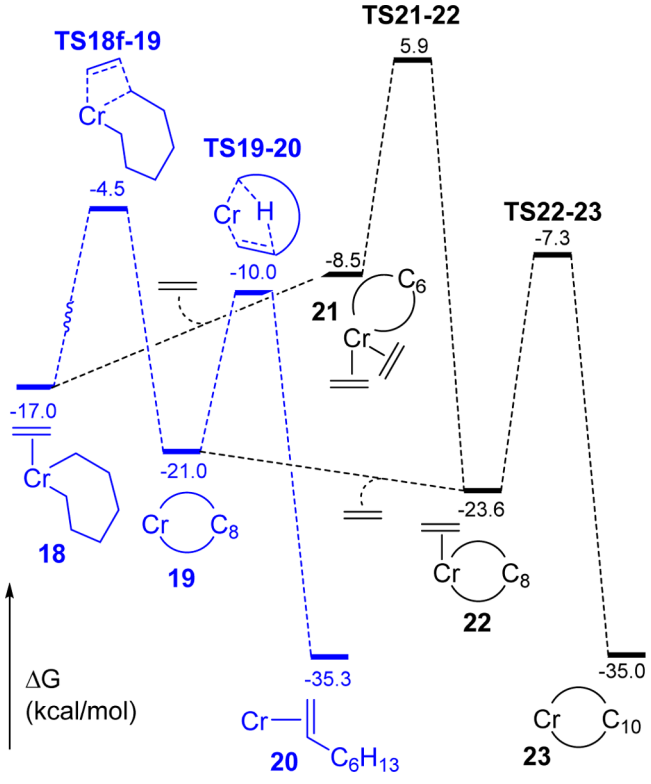

Figure 7. Energy profiles for 1-octene formation versus metallacycle expansion from $[(PNP)Cr(C_6H_{12})(ethylene)]^+$ (**18**). All stationary points shown are cationic. The relative Gibbs free energies (ΔG) obtained from M06L/BS2//M06L/BS1 calculations are given in kcal·mol^{-1}.

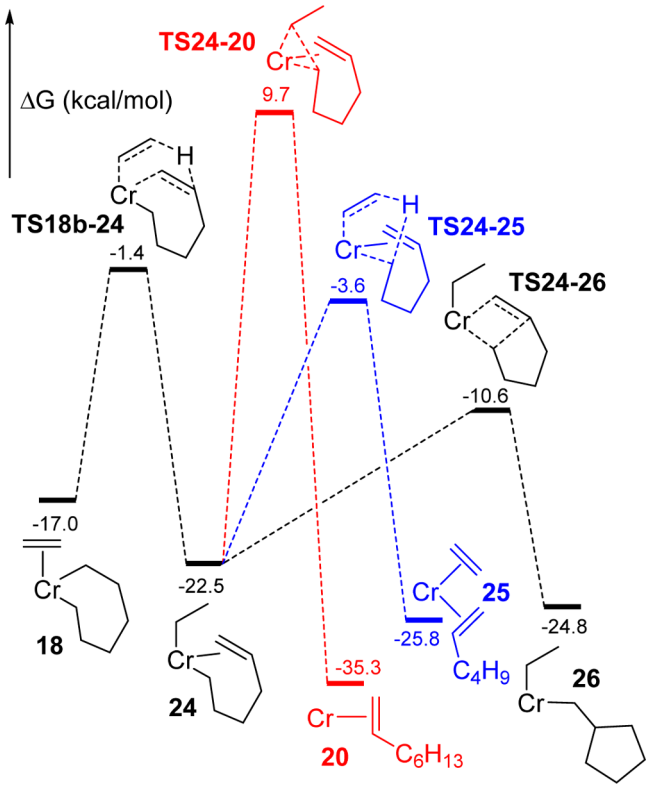

Figure 8. Energy profiles for β-hydride transfer to ethylene and subsequent reaction possibilities from $[(PNP)Cr(C_6H_{12})(ethylene)]^+$ (**18**). All stationary points shown are cationic. The relative Gibbs free energies (ΔG) obtained from M06L/BS2//M06L/BS1 calculations are given in kcal·mol^{-1}.

transformation has previously been observed to occur at a palladium center.[63]

As shown in Figure 9, further β-hydride transfer reactions from complex **26** can lead to both methylcyclopentane and methylenecyclopentane (black pathway), the two most abundant cyclic products formed with this system. The prediction that both products are formed via very similar barrier heights is consistent with the approximate 1:1 ratio found experimentally. Furthermore, ethylene coordination to **26** is also possible, followed by insertion into either of the Cr–alkyl bonds (**TS29-30** or **TS29-31**, blue pathways). This leads to chain extension of either the ethyl or cyclopentylmethyl group. The reaction sequence of either ethylene coordination/insertion or β-hydride transfer can continue from both **30** and **31**. We have calculated the next β-hydride transfer steps from **30** (red pathway), leading to the higher cyclopentane products. The sequence of reactions shown in Figure 9 can therefore explain the range of cyclic products formed with this system and also the distribution of *n*-alkanes (because complex **31** can also eliminate *n*-butane or insert ethylene to produce a longer *n*-alkyl chain). It is noted that the competing barriers for β-hydride transfer (e.g., **TS30-32** versus **TS30-33**) are at almost the same energies and also that the barriers for ethylene insertion are quite similar to those for β-hydride transfer. We return to this point when discussing the correlation between experiment and theory below.

Co-Oligomerization. The cotrimerization and cotetramerization of 1-hexene and 1-octene with ethylene is thought to be responsible for the branched C_{10}–C_{14} coproducts formed in catalysis. Some representative 1-hexene incorporation pathways have been studied, and details are given in the Supporting Information. In brief, the key finding is that metallacycle formation involving 1-hexene to give a metalla(3-butylcyclopentane) complex has a barrier very similar to that involving two ethylene units (for comparison, Labinger and Bercaw recently estimated that ethylene incorporation is 50–70 times faster than α-olefin incorporation[64,65]). Hence, incorporation of 1-hexene and 1-octene into the trimerization and tetramerization process can be rationalized with the theoretical model employed herein.

2.3. Correlation of Experiment and Theory. *Kinetics of 1-Hexene and 1-Octene Formation.* The experimental observation that 1-hexene formation is approximately first-order with respect the ethylene concentration suggests that ethylene is involved in the rate-determining step. This could be either metallacycle formation or metallacyclopentane expansion (ethylene insertion), whereas termination from a metallacycloheptane to give 1-hexene is unlikely to be influenced by ethylene. As noted above, the calculations do not conclusively point to any one step being rate-determining. The barrier heights for metallacycle formation (**TS3-7** or **TS2-6** in Figure 2, 9.1–9.7 kcal·mol^{-1}) are quite similar to that for metallacycle expansion (**TS7-8** in Figure 3, 7.9 kcal·mol^{-1}), which suggests that there is no single rate-determining step. Despite this uncertainty, the transformation from the most stable Cr(I) species, bis(ethylene) complex ^{6}**2**, to chromacycloheptane **8** requires the addition of one ethylene unit, so it is not unreasonable that 1-hexene formation would be first-order in ethylene. In the Supporting Information, we have considered the kinetics of 1-hexene formation in greater detail and show

DOI: 10.1021/acscatal.5b00989
ACS Catal. 2015, 5, 4152–4166

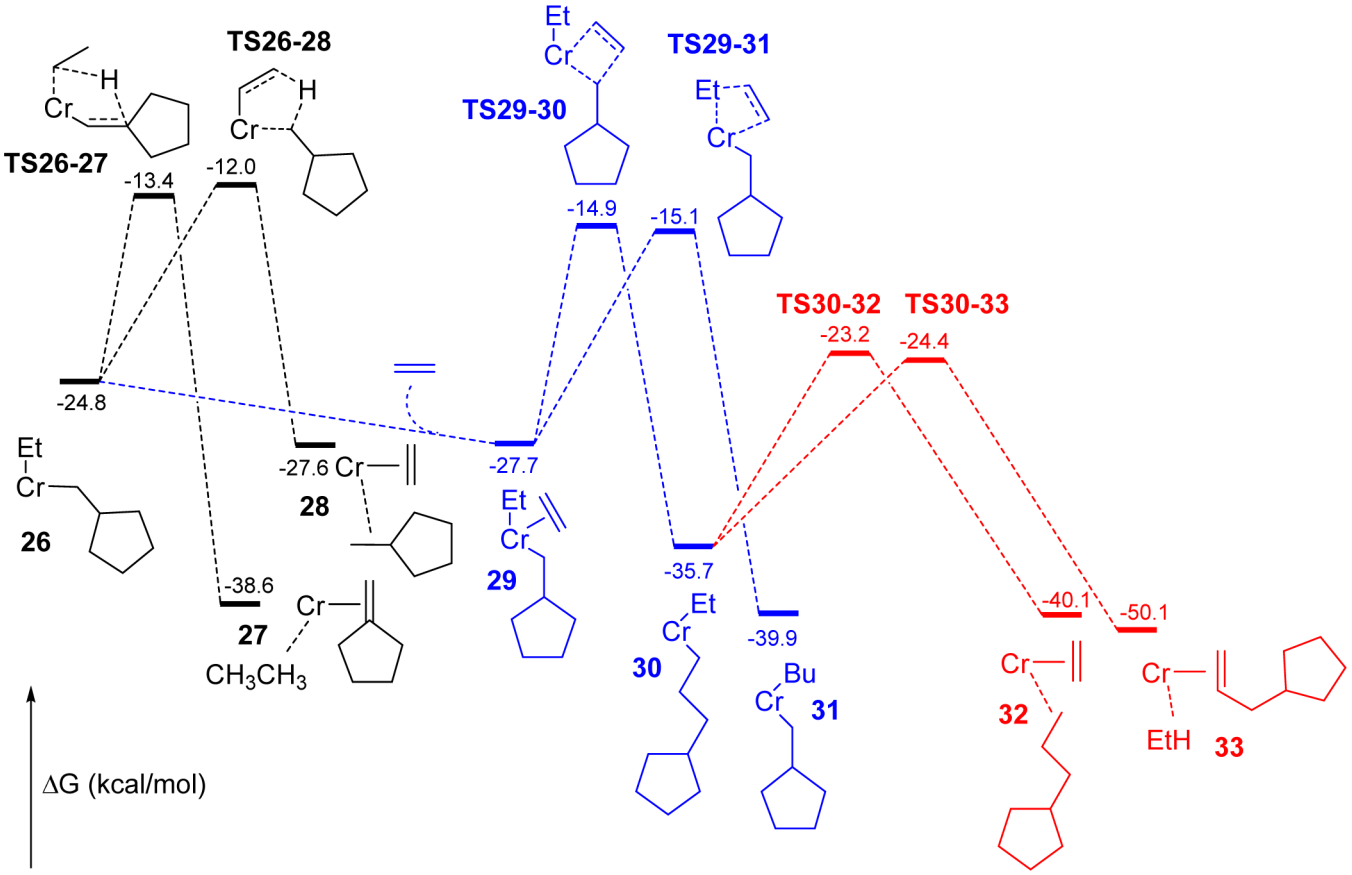

Figure 9. Energy profiles for β-hydride transfer reactions and chain extension from [(PNP)CrEt(cyclopentylmethyl)]$^+$ (**26**). All stationary points shown are cationic. The relative Gibbs free energies (ΔG) obtained from M06L/BS2//M06L/BS1 calculations are given in kcal·mol^{-1}.

how an order in ethylene very close to 1 is found if all products formed via intermediate **8** are combined. This is one possible explanation for the kinetics, but there may be others. As shown in the Supporting Information (Section 10), a 1-hexene dependence that is less than first-order could result simply from the competition between 1-hexene and 1-octene formation, without the need to consider other products formed via **8**.

In terms of 1-octene formation, we propose that the route to 1-octene occurs via both a mono(ethylene) complex **7** and bis(ethylene) complex **17** (Figure 6 and summarized in Scheme 5). The proposed combination of both single- and double-coordination mechanisms[54] can explain the experimentally observed overall order with respect to ethylene of ~1.4 for 1-octene.[36,37] The full rate equation for 1-octene formation according to this possibility is derived in the Supporting Information, section 8. There are possibly other interpretations, which also explain the kinetic observations. For example, if 1-octene is formed only by the bis(ethylene) route, the fractional dependence on ethylene concentration can be explained by a mechanism involving competitive 1-hexene and 1-octene kinetics. This model is illustrated in the Supporting Information (Section 10).

Another possibility that warrants raising is that a double-coordination mechanism may, to a degree, contribute to a proportion of the 1-hexene formation in some cases. As illustrated in Figure 5, two pathways to 1-hexene formation (shown in red) are found with barriers of −0.1 and −0.4 kcal·mol^{-1}. These are very close to the barrier for β-hydride transfer, which ultimately leads to cyclopentanes and *n*-alkanes. A

Scheme 5. Summary of Possible 1-Hexene and 1-Octene Formation Pathways

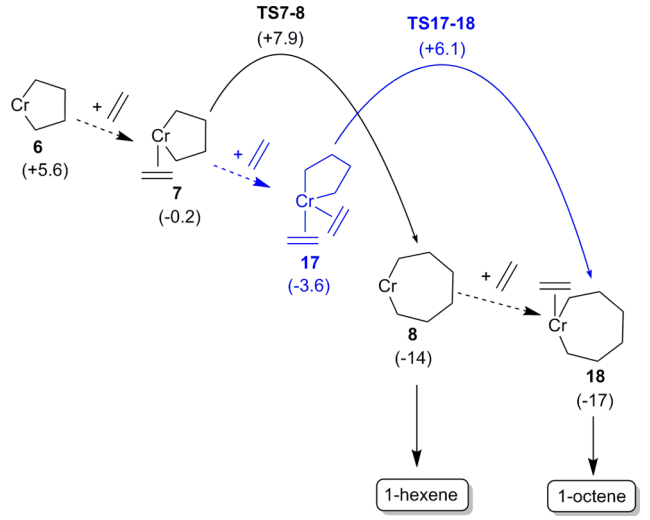

contribution from these routes therefore seems quite possible, although not evident in our experimental results.

Cyclopentanes and n-Alkanes. The formation of cyclopentanes and *n*-alkanes, as shown in Figures 8 and 9, is dependent upon formation of the chromacycloheptane ethylene complex **18**. Although **18** leads mainly to formation of 1-octene, a significant side reaction appears to be β-hydride transfer to ethylene. Like 1-octene, theory predicts that the

DOI: 10.1021/acscatal.5b00989
ACS Catal. 2015, 5, 4152−4166

major routes to these coproducts may involve both single- and double-coordination mechanisms. Therefore, the experimental mixed-order ethylene dependence for cyclopentane formation is consistent with the theoretical predictions, although the existence of a first-order component to alkane formation is not as clear from our data (as shown below, however, the close relationship between cyclopentane and alkane mathematical distributions strongly indicates similar kinetics). This conclusion also explains why the formation of cyclopentanes appears to be associated with tetramerization and not trimerization. The formation of these coproducts effectively limits the maximum selectivity to 1-octene that is achievable; although higher ethylene pressures favor 1-octene formation over 1-hexene, the formation of coproducts is also favored by higher pressure.

Another experimental aspect of this catalyst that can be explained by this mechanistic proposal is the occurrence of hydrogen scrambling in the cyclic products. Prior studies have shown that co-oligomerization of C_2H_4 and C_2D_4 leads to H/D scrambling in the cyclopentanes, despite the absence of such scrambling in 1-hexene and 1-octene.[17] The reason for this becomes clear from the processes presented in Figures 8 and 9. Each of the β-hydride transfer processes shown (β-H to ethylene, β-H to alkyl) involves transfer of a hydrogen to another oligomeric unit. Scrambling of labeled ethylene with the cyclopentanes (and *n*-alkanes) is therefore expected.[66]

The calculated free energy surfaces for formation of the cyclic products can also be used to approximate the distribution of products, and this approximation can be compared to the experimental observations. In theory, the selectivity of competing steps can be calculated from the differences in free energy of activation ($\Delta\Delta G^{\ddagger}$). Although this approach is valid for systems in which chemical accuracy can be obtained, this is certainly not the case with this system.[28] In our opinion, such calculations would imply a level of accuracy in the calculations that is not achievable at this stage. A less quantitative alternative is to make the approximation that very similar barriers are effectively the same and to compare the predictions of this approximation with experiment. Competing barriers for elimination of saturated versus unsaturated cyclopentanes (**TS26-27** vs **TS26-28** and **TS30-32** vs **TS30-33**, Figure 9) were found to be rather similar. As the primary alkyl and alkylcyclopentyl groups grow longer, the two groups will effectively become equivalent, and it might be expected that the barrier heights converge. This effect is illustrated by calculation of both elimination routes from the Cr(*n*-butyl)(cyclopentylpropyl) complex shown in Scheme 6. In this case, the difference in barrier heights, $\Delta\Delta G^{\ddagger}$, is only 0.4 kcal·mol^{-1}. It might therefore be expected that higher cyclic products will have an unsaturated/saturated ratio close to 1. This is found to be the case in our catalysis experiments, with unsaturated/saturated values for C_{10}–C_{20} cyclopentanes observed between 1.0 and 1.1.

The distribution of different chain-length cyclopentanes and *n*-alkanes will be controlled by the rate of elimination versus chain propagation (Figure 9, black pathways versus blue pathways). Again, the calculated barriers are similar. The rate of chain propagation is expected to be influenced by the ethylene concentration, whereas elimination of cyclopentanes or *n*-alkanes is expected to be independent of ethylene. If, at a given concentration of ethylene, the two competing rates are the same, then a Schulz–Flory distribution of these products with a β value[67] of 1.0 would be observed ($\beta = r_{elim}/r_{prop}$).

Scheme 6. β-Hydride Elimination Routes from [(PNP)Cr(*n*-butyl)(Cyclopentylpropyl)]$^+$

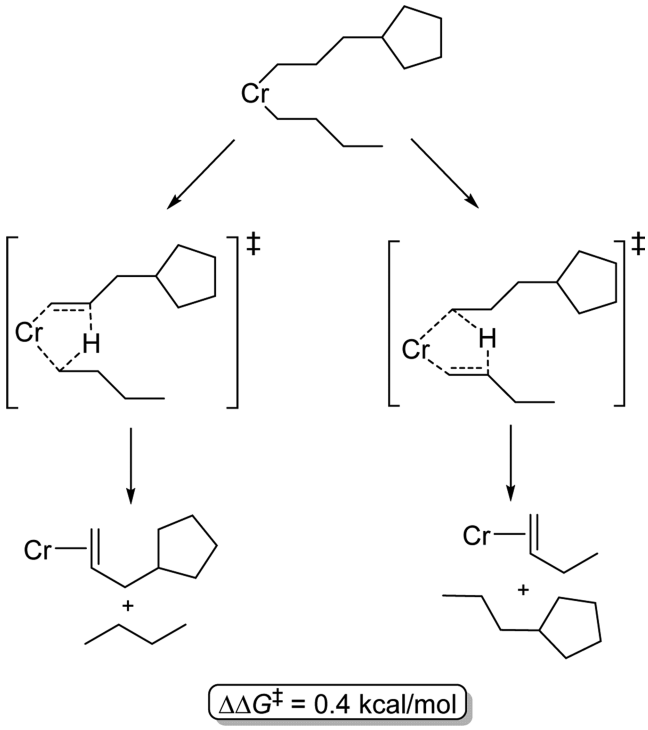

Furthermore, this value should be dependent upon the ethylene pressure, according to our mechanistic model. This is found to be the case, with β values for the cyclopentanes decreasing from 1.3 at 10 bar to 0.6 at 50 bar (see Supporting Information, Table S2). This relationship can, in fact, be analyzed in somewhat greater detail. For a given chromium–dialkyl species, such as **26**, **30**, or **31** in Figure 9, the rate of elimination will be given by $r_{elim} = k_{elim}$[Cr species], whereas the rate of propagation will be $r_{prop} = k_{prop}$[Cr species][C_2H_4]. This leads to the relationship $\beta = k_{elim}/(k_{prop}\cdot[C_2H_4])$, and the Schulz–Flory β value should therefore be proportional to $(P_{ethylene})^{-1}$ according to our model. This is found to be the case for oligomerizations conducted between 20 and 50 bar, although the distribution at 10 bar ethylene pressure deviates significantly from this relationship, as shown in Figure 10. The same relationship is found for the *n*-alkanes (Supporting Information, Figure S16), although again, the data at 10 bar pressure deviates significantly from the linear trend. The reason

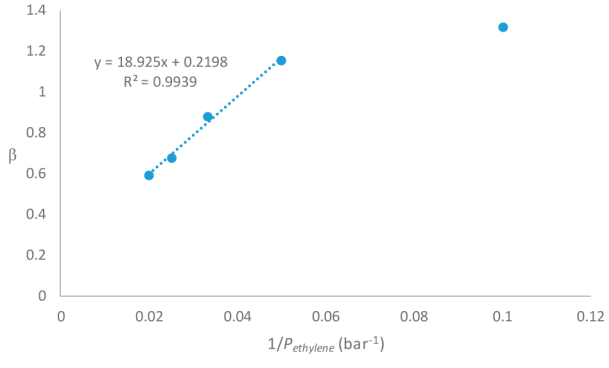

Figure 10. Plot of Schulz–Flory β value of cyclopentane products as a function of ethylene pressure.

DOI: 10.1021/acscatal.5b00989
ACS Catal. 2015, 5, 4152–4166

for this deviation at the lowest pressure is not understood, but overall, the relationship between ethylene pressure and cyclopentanes/*n*-alkanes distribution provides additional support for the proposed mechanism.

A final observation is that the barriers for ethylene insertion into either of the alkyl groups in complex **29** (**TS29-30** or **TS29-31** in Figure 9) are again very similar. If the approximation is made that both of these alternatives have an equal probability, then the amount of C_n alkanes formed should be equal to the C_{n+4} saturated cyclopentanes (e.g., *n*-butane and propylcyclopentane from complexes **30** and **31**). This is found to be approximately the case, with C_n(alkane)/C_{n+4}(saturated cyclic) values of 1.0−1.4 for C_{10}−C_{16} *n*-alkanes. A further consequence of this is that the Schulz−Flory constants for *n*-alkanes and cyclics should be comparable at a given pressure, which is also observed to be the case (see Supporting Information, Table S2).

Selectivity as a Function of Ligand Structure. Although we have considered only a compact methyl-substituted PNP ligand in this work, it is still possible to rationalize the effect of increased steric bulk on the phosphine donors. It is well established that successive introduction of greater steric bulk on the phosphines leads to a shift away from 1-octene generation toward 1-hexene formation instead.[15] This trend continues until 1-octene is almost absent with, for example, *ortho*-^{i}Pr-aryl substitution. We suggest that larger groups will disfavor formation of bis(ethylene) complex **17** and, therefore, retard or completely prevent the double-coordination mechanism. Coordination of a single ethylene unit is still possible, however, and as such, the catalyst becomes a "standard" trimerization system.

The same argument applies with introduction of an additional donor, which is normally in the form of an *ortho*-methoxyaryl substituent.[29,68] Coordination of the ether donor would again prevent coordination of a second ethylene unit, blocking the major tetramerization pathway. The fact that more coordinating counteranions also shift the output toward 1-hexene might be for similar reasons.[69] Investigation of ligand and counterion effects will be the subject of further work.

3. SUMMARY AND CONCLUSION

Herein, we have reported a detailed experimental and theoretical study of the Cr-PNP ethylene tetramerization system. The total product output of the catalyst has been analyzed, and it has been found that, along with 1-octene, the coproducts cyclopentanes, *n*-alkanes, and higher LAOs display a partial second-order response to ethylene concentration. Theoretical studies have been employed to elucidate the likely mechanism. The resultant mechanistic proposal displays excellent overall correlation between experiment and theory, which lends support for a mechanism that involves a monometallic, formally cationic catalyst that shuttles between Cr(I) and Cr(III) oxidation states. We note that the mechanistic model developed herein correlates well with not only our experiments but also the bulk of existing experimental data on these systems.

A key feature of the mechanism is that 1-hexene results predominately from a mono(ethylene) chromacyclopentane intermediate, whereas 1-octene formation proceeds via a bis(ethylene) metallacyclic complex, possibly with additional involvement of a mono(ethylene) pathway. The relatively unique ability of this system to catalyze tetramerization with high selectivity appears to arise from the bidentate PNP ligand, which allows coordination of a fourth ethylene unit. Although a related double-coordination mechanism has previously been proposed to explain kinetics and isospecificity in α-olefin polymerization,[54] we have shown here that this concept also explains the highly selective formation of 1-octene. This mechanism not only leads to 1-octene but also accounts for the side reactions to cyclopentanes and *n*-alkanes. This latter point explains the general observation that trimerization catalysis often proceeds with high selectivity and far fewer coproducts produced. A number of trimerization systems are capable of 1-hexene selectivities well over 90%,[5,6,8] with the major coproducts being the cotrimers of 1-hexene and ethylene. Co-oligomerization is a secondary process that can occur to a greater or lesser extent with any trimerization or tetramerization catalyst. On the other hand, Schulz−Flory distributions of cyclopentanes and alkanes result from the same intermediates as tetramerization, and are therefore linked to 1-octene formation. This conclusion appears to accord well with experimental observations.

Although not studied as part of this work, it is worth commenting on an alternative mechanistic proposal for 1-octene formation, the bimetallic mechanism.[27] This proposal invokes the coupling of two metallacyclopentane rings in a binuclear chromium complex, which then leads to 1-octene elimination. The formation of 1-hexene is proposed to occur via the standard mononuclear metallacycle mechanism, and the selectivity to 1-octene or 1-hexene is therefore controlled by the catalyst speciation (bi- or mononuclear). To our knowledge, the only systematic study addressing the possibility of a binuclear catalyst was that carried out by Theopold and co-workers.[70] They concluded that a bimetallic mechanism is unlikely, favoring instead a monometallic catalyst. It is also noted that 1-hexene/1-octene selectivity with the Cr-PNP system is not affected by changes in the concentration of chromium; both products follow first-order kinetics with respect to chromium. Support for a bimetallic mechanism appears to result more from the idea that a monometallic mechanism cannot explain 1-octene formation, rather than from experimental evidence for it. We have shown herein that not only 1-octene but also all coproducts can be fully explained by a monometallic mechanism. Lacking new evidence to the contrary, we believe the monometallic mechanistic model presented herein is most likely.

We are currently studying ligand and cocatalyst (anion) influences on the tetramerization reaction, as well as studying the full scope of the double-coordination mechanism in metallacyclic oligomerization. Results of this work will be published in due course.

■ ASSOCIATED CONTENT

Supporting Information

The Supporting Information is available free of charge on the ACS Publications website at DOI: 10.1021/acscatal.5b00989.

Optimized geometries of all stationary points (XYZ)
Experimental and theoretical methods, plots of product formation as a function of pressure (reaction order determination), investigation of synchronous ethylene coupling and concerted double insertion pathways, investigation of 1-hexene/ethylene cotrimerization, further discussion of kinetics of 1-hexene and 1-octene formation, and analysis of carbon number distribution of cyclopentanes and alkanes (PDF)

DOI: 10.1021/acscatal.5b00989
ACS Catal. 2015, 5, 4152−4166

AUTHOR INFORMATION

Corresponding Authors

*E-mail: g.britovsek@imperial.ac.uk.
*E-mail: david.mcguinness@utas.edu.au.

Notes

The authors declare no competing financial interest.

ACKNOWLEDGMENTS

We thank the Australian Research Council for financial support through Grant FT100100609 to D.S.M. and the University of Tasmania for Visiting Scholars funding to G.J.P.B. The Australian National Computational Infrastructure scheme and the Tasmanian Partnership for Advanced Computing are thanked for provision of computing resources. We thank Professor B. F. Yates and Dr. Bun Chan for advice and Professor J. N. Harvey for providing the minimum energy crossing point calculation code.

REFERENCES

(1) Forestière, A.; Olivier-Bourbigou, H.; Saussine, L. *Oil Gas Sci. Technol.* **2009**, *64*, 649−667.
(2) Olivier-Bourbigou, H.; Forestière, A.; Saussine, L.; Magna, L.; Favre, F.; Hugues, F. *Oil Gas Eur. Mag.* **2010**, *36*, 97−102.
(3) Belov, G. P.; Matkovsky, P. E. *Pet. Chem.* **2010**, *50*, 283−289.
(4) Keim, W. *Angew. Chem., Int. Ed.* **2013**, *52*, 12492−12496.
(5) McGuinness, D. S. *Chem. Rev.* **2011**, *111*, 2321−2341.
(6) Agapie, T. *Coord. Chem. Rev.* **2011**, *255*, 861−880.
(7) van Leeuwen, P. W. N. M.; Clément, N. D.; Tschan, M. J.-L. *Coord. Chem. Rev.* **2011**, *255*, 1499−1517.
(8) Dixon, J. T.; Green, M. J.; Hess, F. M.; Morgan, D. H. J. *J. Organomet. Chem.* **2004**, *689*, 3641−3669.
(9) Wass, D. F. *Dalton Trans.* **2007**, 816−819.
(10) Bollmann, A.; Blann, K.; Dixon, J. T.; Hess, F. M.; Killian, E.; Maumela, H.; McGuinness, D. S.; Morgan, D. H.; Neveling, A.; Otto, S.; Overett, M.; Slawin, A. M. Z.; Wasserscheid, P.; Kuhlmann, S. J. *J. Am. Chem. Soc.* **2004**, *126*, 14712−14713.
(11) Overett, M. J.; Blann, K.; Bollmann, A.; de Villiers, R.; Dixon, J. T.; Killian, E.; Maumela, M. C.; Maumela, H.; McGuinness, D. S.; Morgan, D. H.; Rucklidge, A.; Slawin, A. M. Z. J. *J. Mol. Catal. A: Chem.* **2008**, *283*, 114−119.
(12) Sydora, O. L.; Jones, T. C.; Small, B. L.; Nett, A. J.; Fischer, A. A.; Carney, M. J. *ACS Catal.* **2012**, *2*, 2452−2455.
(13) Shaikh, Y.; Albahily, K.; Sutcliffe, M.; Fomitcheva, V.; Gambarotta, S.; Korobkov, I.; Duchateau, R. *Angew. Chem., Int. Ed.* **2012**, *51*, 1366−1369.
(14) Yang, Y.; Liu, Z.; Liu, B.; Duchateau, R. *ACS Catal.* **2013**, *3*, 2353−2361.
(15) Blann, K.; Bollmann, A.; Dixon, J. T.; Hess, F.; Killian, E.; Maumela, H.; Morgan, D. H.; Neveling, A.; Otto, S.; Overett, M. *Chem. Commun.* **2005**, 620−621.
(16) Agapie, T.; Schofer, S. J.; Labinger, J. A.; Bercaw, J. E. J. *J. Am. Chem. Soc.* **2004**, *126*, 1304−1305.
(17) Overett, M. J.; Blann, K.; Bollmann, A.; Dixon, J. T.; Haasbroek, D.; Killian, E.; Maumela, H.; McGuinness, D. S.; Morgan, D. H. J. *J. Am. Chem. Soc.* **2005**, *127*, 10723−10730.
(18) Schofer, S. J.; Day, M. W.; Henling, L. M.; Labinger, J. A.; Bercaw, J. E. *Organometallics* **2006**, *25*, 2743−2749.
(19) Agapie, T.; Labinger, J. A.; Bercaw, J. E. J. *J. Am. Chem. Soc.* **2007**, *129*, 14281−14295.
(20) Janse van Rensburg, W.; van den Berg, J.-A.; Steynberg, P. J. *Organometallics* **2007**, *26*, 1000−1013.
(21) Jabri, A.; Crewdson, P.; Gambarotta, S.; Korobkov, I.; Duchateau, R. *Organometallics* **2006**, *25*, 715−718.
(22) Rucklidge, A. J.; McGuinness, D. S.; Tooze, R. P.; Slawin, A. M. Z.; Pelletier, J. D. A.; Hanton, M. J.; Webb, P. B. *Organometallics* **2007**, *26*, 2782−2787.
(23) Bowen, L. E.; Haddow, M. F.; Orpen, A. G.; Wass, D. F. *Dalton Trans.* **2007**, 1160−1168.
(24) Brückner, A.; Jabor, J. K.; McConnell, A. E. C.; Webb, P. B. *Organometallics* **2008**, *27*, 3849−3856.
(25) Rabeah, J.; Bauer, M.; Baumann, W.; McConnell, A. E.; Gabrielli, W. F.; Webb, P. B.; Selent, D.; Brückner, A. *ACS Catal.* **2013**, *3*, 95−102.
(26) Do, L. H.; Labinger, J. A.; Bercaw, J. E. *ACS Catal.* **2013**, *3*, 2582−2585.
(27) Peitz, S.; Aluri, B. R.; Peulecke, N.; Müller, B. H.; Wöhl, A.; Müller, W.; Al-Hazmi, M. H.; Mosa, F. M.; Rosenthal, U. *Chem. - Eur. J.* **2010**, *16*, 7670−7676.
(28) McGuinness, D. S.; Chan, B.; Britovsek, G. J. P.; Yates, B. F. *Aust. J. Chem.* **2014**, *67*, 1481−1490.
(29) Carter, A.; Cohen, S. A.; Cooley, N. A.; Murphy, A.; Scutt, J.; Wass, D. F. *Chem. Commun.* **2002**, 858−859.
(30) Kuhlmann, S.; Blann, K.; Bollmann, A.; Dixon, J. T.; Killian, E.; Maumela, M. C.; Maumela, H.; Morgan, D. H.; Prétorius, M.; Taccardi, N.; Wasserscheid, P. J. *J. Catal.* **2007**, *245*, 279−284.
(31) Killian, E.; Blann, K.; Bollmann, A.; Dixon, J. T.; Kuhlmann, S.; Maumela, M. C.; Maumela, H.; Morgan, D. H.; Nongodlwana, P.; Overett, M.; Pretorius, M.; Höfener, K.; Wasserscheid, P. J. *J. Mol. Catal. A: Chem.* **2007**, *270*, 214−218.
(32) Suttil, J. A.; Wasserscheid, P.; McGuinness, D. S.; Gardiner, M. G.; Evans, S. J. *Catal. Sci. Technol.* **2014**, *4*, 2574−2588.
(33) Hey, T. W.; Wass, D. F. *Organometallics* **2010**, *29*, 3676−3678.
(34) Bowen, L. E.; Wass, D. F. *Organometallics* **2006**, *25*, 555−557.
(35) Bowen, L. E.; Charernsuk, M.; Hey, T. W.; McMullin, C. L.; Orpen, A. G.; Wass, D. F. *Dalton Trans.* **2010**, *39*, 560−567.
(36) Walsh, R.; Morgan, D. H.; Bollmann, A.; Dixon, J. T. *Appl. Catal., A* **2006**, *306*, 184−191.
(37) Kuhlmann, S.; Paetz, C.; Hägele, C.; Blann, K.; Walsh, R.; Dixon, J. T.; Scholz, J.; Haumann, M.; Wasserscheid, P. J. *J. Catal.* **2009**, *262*, 83−91.
(38) Kuhlmann, S.; Dixon, J. T.; Haumann, M.; Morgan, D. H.; Ofili, J.; Spuhl, O.; Taccardi, N.; Wasserscheid, P. *Adv. Synth. Catal.* **2006**, *348*, 1200−1206.
(39) Blann, K.; Bollmann, A.; Dixon, J. T.; Neveling, A.; Morgan, D. H.; Maumela, H.; Killian, E.; Hess, F.; Otto, S.; Pepler, L.; Mahomed, H.; Overett, M. WO 2004/056479 (Sasol Technology) 2004.
(40) The possibility of a transition structure involving synchronous coupling of three ethylene units to form a chromacycloheptane in one step was considered, but found not to be energetically competitive. Details are provided in the Supporting Information.
(41) Harvey, J. N.; Aschi, M.; Schwarz, H.; Koch, W. *Theor. Chem. Acc.* **1998**, *99*, 95−99.
(42) McDermott, J. X.; White, J. F.; Whitesides, G. M. J. *J. Am. Chem. Soc.* **1973**, *95*, 4451−4452.
(43) McDermott, J. X.; White, J. F.; Whitesides, G. M. J. *J. Am. Chem. Soc.* **1976**, *98*, 6521−6528.
(44) McDermott, J. X.; Wilson, M. E.; Whitesides, G. M. J. *J. Am. Chem. Soc.* **1976**, *98*, 6529−6536.
(45) Blok, A. N. J.; Budzelaar, P. H. M.; Gal, A. W. *Organometallics* **2003**, *22*, 2564−2570.
(46) de Bruin, T. J. M.; Magna, L.; Raybaud, P.; Toulhoat, H. *Organometallics* **2003**, *22*, 3404.
(47) Tobisch, S.; Ziegler, T. *Organometallics* **2003**, *22*, 5392−5405.
(48) Robinson, R.; McGuinness, D. S.; Yates, B. F. *ACS Catal.* **2013**, *3*, 3006−3015.
(49) Tobisch, S.; Ziegler, T. J. *J. Am. Chem. Soc.* **2004**, *126*, 9059−9071.
(50) Yang, Y.; Liu, Z.; Zhong, L.; Qiu, P.; Dong, Q.; Cheng, R.; Vanderbilt, J.; Liu, B. *Organometallics* **2011**, *30*, 5297−5302.
(51) Qi, Y.; Dong, Q.; Zhong, L.; Liu, Z.; Qiu, P.; Cheng, R.; He, X.; Vanderbilt, J.; Liu, B. *Organometallics* **2010**, *29*, 1588−1602.
(52) Budzelaar, P. H. M. *Can. J. Chem.* **2009**, *87*, 832−837.
(53) Ystenes, M. J. *J. Catal.* **1991**, *129*, 383−401.
(54) Marques, M. M.; Dias, A. R.; Costa, C.; Lemos, F.; Ramôa Ribeira, F. *Polym. Int.* **1997**, *43*, 77−85.

DOI: 10.1021/acscatal.5b00989
ACS Catal. 2015, 5, 4152−4166

(55) Kelly, W. M.; Wang, S.; Collins, S. *Macromolecules* **1997**, *30*, 3151−3158.
(56) While potential energy scans lead to an energy maximum between 18b and 18d, we were unable to optimize to a corresponding transition structure. This is likely because the potential energy surface is very flat within the proximity of 18d (the energy maximum is only 1.0 kcal mol^{-1} above 18d).
(57) Tomov, A. K.; Chirinos, J. J.; Jones, D. J.; Long, R. J.; Gibson, V. C. J. *J. Am. Chem. Soc.* **2005**, *127*, 10166−10167.
(58) Tomov, A. K.; Gibson, V. C.; Britovsek, G. J. P.; Long, R. J.; van Meurs, M.; Jones, D. J.; Tellmann, K. P.; Chirinos, J. J. *Organometallics* **2009**, *28*, 7033−7040.
(59) Tomov, A. K.; Chirinos, J. J.; Long, R. J.; Gibson, V. C.; Elsegood, M. R. J. J. *J. Am. Chem. Soc.* **2006**, *128*, 7704−7705.
(60) Tenza, K.; Hanton, M. J.; Slawin, A. M. Z. *Organometallics* **2009**, *28*, 4852−4867.
(61) McGuinness, D. S.; Suttil, J. A.; Gardiner, M. G.; Davies, N. W. *Organometallics* **2008**, *27*, 4238−4247.
(62) Just as in Figure 5, there are a number of different isomers of the intermediates shown in Figure 7, which lead to different transition structure geometries. For the sake of clarity, only the lowest-energy routes are shown in Figure 7.
(63) Perch, N. S.; Widenhoefer, R. A. *Organometallics* **2001**, *20*, 5251−5253.
(64) Do, L. H.; Labinger, J. A.; Bercaw, J. E. *Organometallics* **2012**, *31*, 5143−5149.
(65) Sattler, A.; Labinger, J. A.; Bercaw, J. E. *Organometallics* **2013**, *32*, 6899−6902.
(66) The mechanism of cyclopentane and alkane formation will also lead to a secondary distribution of α-olefins, in which scrambling of labeled ethylene would result. As such, a small amount of scrambled 1-hexene and 1-octene is expected.
(67) The β value used here ($= r_{elim}/r_{prop}$) is related to the Schulz−Flory K value by $K = (\text{mol } C_{n+2}/\text{mol } C_n) = (1 + \beta)^{-1}$.
(68) Overett, M. J.; Blann, K.; Bollmann, A.; Dixon, J. T.; Hess, F. M.; Killian, E.; Maumela, H.; Morgan, D. H.; Neveling, A.; Otto, S. *Chem. Commun.* **2005**, 622−624.
(69) McGuinness, D. S.; Rucklidge, A. J.; Tooze, R. P.; Slawin, A. M. Z. *Organometallics* **2007**, *26*, 2561−2569.
(70) Monillas, W. H.; Young, J. F.; Yap, G. P. A.; Theopold, K. H. *Dalton Trans.* **2013**, *42*, 9198−9210.

DOI: 10.1021/acscatal.5b00989
ACS Catal. 2015, 5, 4152−4166